

# Efficient Low-Rank Matrix Learning by Factorizable Nonconvex Regularization

Yaqing Wang<sup>1</sup> Quanming Yao<sup>2\*</sup> James T. Kwok<sup>3</sup>

<sup>1</sup>Baidu Research (Beijing)

<sup>2</sup>4Paradigm Inc (Hong Kong)

<sup>3</sup>Department of Computer Science, Hong Kong University of Science and Technology

## Abstract

Matrix learning is at the core of many machine learning problems. To encourage a low-rank matrix solution, besides using the traditional convex nuclear norm regularizer, a popular recent trend is to use nonconvex regularizers that adaptively penalize singular values. They offer better recovery performance, but require computing the expensive singular value decomposition (SVD) in each iteration. To remove this bottleneck, we consider the "nuclear norm minus Frobenius norm" regularizer. Besides having nice theoretical properties on recovery and shrinkage as the other nonconvex regularizers, it can be reformulated into a factorized form that can be efficiently optimized by gradient-based algorithms while avoiding the SVD computations altogether. Extensive low-rank matrix completion experiments on a number of synthetic and real-world data sets show that the proposed method obtains state-of-the-art recovery performance and is much more efficient than existing low-rank convex / nonconvex regularization and matrix factorization algorithms.

## 1 Introduction

Matrix learning is a fundamental tool in machine learning [1, 8, 19, 28]. It has been widely used on a number of tasks such as matrix completion [8], robust principal component analysis [5], multitask learning [9] and subspace clustering [20]. To avoid the problem to be ill-posed, the target matrix is often assumed to have a low rank [6]. However, rank minimization is NP-hard [6]. Thus, computationally, a more feasible approach is to use a regularizer that encourages the target matrix to be low-rank. A popular choice is the nuclear norm regularizer, which is convex and is the tightest convex surrogate of the matrix rank [6]. However, intuitively, larger singular values carry more information, and so should be shrunk less. Along this direction, many nonconvex low-rank regularizers have been recently proposed. Common examples include the capped- $\ell_1$  penalty [35], log-sum penalty (LSP) [8], and minimax concave penalty (MCP) [34]. Empirically, they obtain much better recovery performance than the nuclear norm regularizer. Theoretically, they also offer better statistical recovery guarantees [14].

Because of the more complicated forms of these nonconvex low-rank regularizers, their subsequent optimization problems are more difficult and computationally inefficient. In particular, as these regularizers manipulate each singular value adaptively, singular value decomposition (SVD) needs to be computed in each iteration of the optimization process. However, SVD computation scales cubically with the matrix size, which is expensive on large matrices.

To alleviate this problem, we revisit a special case of a recent nonconvex regularizer called the truncated  $\ell_{1-2}$  regularizer [22]. We show that it can adaptively shrink the singular values (with the larger singular values being shrunk less) as existing low-rank nonconvex regularizers. However, existing solver for this truncated  $\ell_{1-2}$  regularizer is very computationally expensive, and requires the

\*Correspondence to Q. Yao at: [yaoquanming@4paradigm.com](mailto:yaoquanming@4paradigm.com).

combined use of the difference of convex functions algorithm (DCA) [16] and the alternating direction method of multipliers (ADMM) [2]. We propose a reformulation of this regularizer in factorized matrix form. Besides having nice theoretical properties under the restricted isometry property, a major advantage of the resultant low-rank model is that it can be efficiently optimized by gradient descent, while avoiding the expensive SVD altogether. Extensive experiments are performed on an important class of low-rank matrix learning problems, namely matrix completion [?, 6]. A number of synthetic and real-world recommendation / hyperspectral / climate data sets are used. Results consistently show that the proposed algorithm obtains state-of-the-art recovery performance as the other nonconvex regularizers, but can be orders of magnitude faster on large data sets.

**Notations:** In the sequel, vectors are denoted by lowercase boldface, matrices by uppercase boldface, and the transpose by the superscript  $(\cdot)^\top$ . For a vector  $\mathbf{x} = [x_i] \in \mathbb{R}^m$ ,  $\text{Diag}(\mathbf{x})$  constructs a  $m \times m$  diagonal matrix with the  $i$ th diagonal element being  $x_i$ .  $\mathbf{I}$  denotes the identity matrix. For a square matrix  $\mathbf{X}$ ,  $\text{tr}(\mathbf{X})$  is its trace. For matrix  $\mathbf{X} \in \mathbb{R}^{m \times n}$  (without loss of generality, we assume that  $m \geq n$ ),  $\|\mathbf{X}\|_F = \sqrt{\text{tr}(\mathbf{X}^\top \mathbf{X})}$  is its Frobenius norm. Let the singular value decomposition (SVD) of  $\mathbf{X}$  be  $\mathbf{U}\text{Diag}(\boldsymbol{\sigma}(\mathbf{X}))\mathbf{V}^\top$ , where  $\mathbf{U} \in \mathbb{R}^{m \times k^*}$ ,  $\mathbf{V} \in \mathbb{R}^{n \times k^*}$ ,  $k^*$  is the rank of  $\mathbf{X}$ ,  $\boldsymbol{\sigma}(\mathbf{X}) = [\sigma_i(\mathbf{X})] \in \mathbb{R}^{k^*}$  with  $\sigma_i(\mathbf{X})$  being the  $i$ th singular value of  $\mathbf{X}$  and  $\sigma_1(\mathbf{X}) \geq \sigma_2(\mathbf{X}) \geq \dots \geq \sigma_{k^*}(\mathbf{X}) \geq 0$ .

## 2 Background: Low-Rank Matrix Learning

As minimizing the rank is NP-hard [6], low-rank matrix learning is often formulated as the following optimization problem:

$$\min f(\mathbf{X}) + \lambda r(\mathbf{X}), \quad (1)$$

where  $f$  is a smooth function (usually the loss),  $r(\mathbf{X})$  is a regularizer that encourages  $\mathbf{X}$  to be low-rank, and  $\lambda \geq 0$  is a tradeoff hyperparameter. The most popularly used low-rank regularizer is based on the nuclear norm  $\|\mathbf{X}\|_* = \|\boldsymbol{\sigma}(\mathbf{X})\|_1$  [6], which is also the tightest convex surrogate of the matrix rank [11]. Problem (1) is usually solved by the proximal algorithm [25]. At the  $t$ th iteration, it generates the next iterate by computing the proximal step  $\mathbf{X}_{t+1} = \text{prox}_{\eta\lambda r}(\mathbf{X}_t - \eta\lambda \nabla f(\mathbf{X}_t))$ , where  $\eta > 0$  is the stepsize, and  $\text{prox}_{\lambda r}(\mathbf{Z}) = \arg \min_{\mathbf{X}} \frac{1}{2} \|\mathbf{X} - \mathbf{Z}\|_2^2 + \lambda r(\mathbf{X})$  is the proximal operator. In general, the proximal operator should be easily computed. For the nuclear norm, its proximal operator is computed as [4]:

$$\text{prox}_{\lambda \|\cdot\|_*}(\mathbf{Z}) = \mathbf{U} (\text{Diag}(\boldsymbol{\sigma}(\mathbf{Z})) - \lambda \mathbf{I})_+ \mathbf{V}^\top, \quad (2)$$

where  $\mathbf{U}\text{Diag}(\boldsymbol{\sigma}(\mathbf{Z}))\mathbf{V}^\top$  is the singular value decomposition (SVD) of  $\mathbf{Z}$ , and  $\mathbf{A}_+ = [\max(A_{ij}, 0)]$ .

While the proximal operator in (2) penalizes all singular values of  $\mathbf{Z}$  by the same amount  $\lambda$ , the larger singular values should intuitively be more informative and thus penalized less. This leads to the recent development of a number of nonconvex regularizers. Common examples include the capped- $\ell_1$  penalty [35], log-sum penalty (LSP) [8], and minimax concave penalty (MCP) [34]. They can be written in the general form of

$$r(\mathbf{X}) = \sum_{i=1}^n \hat{r}(\sigma_i(\mathbf{X})), \quad (3)$$

where  $\hat{r}(\alpha)$  is nonlinear, concave and non-decreasing for  $\alpha \geq 0$  with  $\hat{r}(0) = 0$ . A recent addition is the truncated  $\ell_{1-2}$  regularizer [22]:

$$\ell_{t,1-2}(\boldsymbol{\sigma}(\mathbf{X})) \equiv \sum_{i=t+1}^n \sigma_i(\mathbf{X}) - \sqrt{\sum_{i=t+1}^n \sigma_i^2(\mathbf{X})}, \quad (4)$$

which keeps the  $t$  largest singular values of the matrix argument intact and only penalizes the remaining ones. It is advantageous in being unbiased, in the sense that  $\ell_{t,1-2}(\boldsymbol{\sigma}(\mathbf{X})) = 0$  if and only if  $\mathbf{X}$  has rank  $t + 1$  [22]. Empirically, nonconvex regularizers outperform the (convex) nuclear norm regularizer on many low-rank matrix learning applications such as image inpainting [13], collaborative filtering [21, 30] and background modeling [33]. Moreover, it can be shown theoretically that they obtain lower recovery errors than the nuclear norm regularizer [8, 34, 35].

Note that all these nonconvex regularizers require access to individual singular values. As computing the singular values of a  $m \times n$  matrix (with  $m \geq n$ ) via SVD takes  $O(mn^2)$  time, this can be costly

for a large matrix. Even when rank- $k$  truncated SVD is used, the computation cost is still  $O(mnk)$ , and can be problematic when both  $m$  and  $n$  are large. Moreover, learning with these nonconvex regularizers is more difficult, and dedicated solvers are needed to leverage special structures (such as the low-rank-plus-sparse structure in [15, 33]). In particular, to solve the truncated  $\ell_{1-2}$  regularized problem, one has to first use the difference of convex functions algorithm (DCA) [16] to decompose the nonconvex regularizer, and then solve the subproblems by the alternating direction method of multipliers (ADMM) [2]. These makes its optimization even slower than those of the other nonconvex regularizers.

### 3 Nuclear Norm Minus Frobenius Norm Regularizer

In this paper, we propose an efficient nonconvex regularization solver that bypasses the necessity of performing SVD in each iteration. First, note that while the truncated  $\ell_{1-2}$  regularizer is unbiased when setting its  $t$  value to  $k - 1$  for a desired matrix rank of  $k$ , setting  $t$  this way cannot yield satisfactory performance in practice. A heuristic scheme is adopted in [22] to find an appropriate  $t$ .

In this paper, we sidestep this issue by simply setting  $t = 0$  in (4), leading to:

$$r_{\text{NNFN}}(\mathbf{X}) = \sum_{i=1}^n \sigma_i(\mathbf{X}) - \sqrt{\sum_{i=1}^n \sigma_i^2(\mathbf{X})} = \|\mathbf{X}\|_* - \|\mathbf{X}\|_F. \quad (5)$$

In the sequel, this will be called the “nuclear norm minus Frobenius norm” (NNFN) regularizer. In Section 3.1, we will first show some nice theoretical properties that are still exhibited by this NNFN regularizer. Moreover, interestingly, a major advantage of this NNFN regularizer is that it can be used with a factored matrix form to facilitate efficient optimization (Section 3.2).

#### 3.1 Theoretical Properties

Although the NNFN regularizer is unbiased only for rank-one matrices, stable recovery is guaranteed for matrices of any rank [22].

**Proposition 3.1** ([22]). *With  $f(\mathbf{X}) = \frac{1}{2}\|\mathcal{A}(\mathbf{X}) - \mathbf{b}\|_2^2$ , where  $\mathcal{A}$  is an affine transform satisfying the restricted isometry property (RIP)<sup>2</sup>, and  $\mathbf{b} = \mathcal{A}(\mathbf{X}^*) + \mathbf{e}$  is a measurement vector corresponding to a rank- $k^*$  matrix  $\mathbf{X}^*$  and error vector  $\mathbf{e}$ . Let  $\mathbf{X}$  be the critical point of the equivalent constrained formulation of (1) with NNFN regularization:  $\arg \min_{\mathbf{X}} f(\mathbf{X})$  s.t.  $r_{\text{NNFN}}(\mathbf{X}) \leq \beta$ , where  $\beta \geq 0$  is a hyperparameter. Then,  $\|\mathbf{X} - \mathbf{X}^*\|_F \leq c\|\mathbf{e}\|_2$  for some constant  $c$ .*

Another nice property of the NNFN regularizer is provable adaptive shrinkage of the singular values when used with a proximal algorithm. First, the following Proposition shows that the proximal operator of  $r_{\text{NNFN}}(\cdot)$  can be easily obtained from the corresponding proximal operator  $\text{prox}_{\lambda\|\cdot\|_{1-2}}(\cdot)$  of the  $\ell_{1-2}$  regularizer. All the proofs are in Appendix A.

**Proposition 3.2.** *Given a matrix  $\mathbf{Z}$ , let its SVD be  $\bar{\mathbf{U}}\text{Diag}(\boldsymbol{\sigma}(\mathbf{Z}))\bar{\mathbf{V}}^\top$ , and  $\lambda \leq \|\boldsymbol{\sigma}(\mathbf{Z})\|_\infty$ .*

$$\text{prox}_{\lambda r_{\text{NNFN}}}(\mathbf{Z}) = \bar{\mathbf{U}}\text{Diag}(\text{prox}_{\lambda\|\cdot\|_{1-2}}(\boldsymbol{\sigma}(\mathbf{Z})))\bar{\mathbf{V}}^\top, \quad (6)$$

where  $\text{prox}_{\lambda\|\cdot\|_{1-2}}(\mathbf{z}) = \bar{\mathbf{z}}(\|\bar{\mathbf{z}}\|_2 + \lambda)/\|\bar{\mathbf{z}}\|_2$  with  $\bar{\mathbf{z}} = \text{prox}_{\lambda\|\cdot\|_1}(\mathbf{z}) = \text{sign}(\mathbf{z}) \odot \max(|\mathbf{z}| - \lambda, 0)$  being the soft thresholding operator [10].

As is well-known, the soft thresholding operator leads to a sparse  $\text{prox}_{\lambda\|\cdot\|_{1-2}}(\boldsymbol{\sigma}(\mathbf{Z}))$ , and so  $\text{prox}_{\lambda r_{\text{NNFN}}}(\mathbf{Z})$  is low-rank. Recall from (2) that the proximal operator of the nuclear norm equally penalizes each singular value by  $\lambda$  until it reaches zero. The following Proposition shows that  $\text{prox}_{\lambda r_{\text{NNFN}}}(\cdot)$  adaptively shrinks the singular values of its matrix argument, in that larger singular values are penalized less.

**Proposition 3.3.** *Let  $\tilde{\boldsymbol{\sigma}} = [\tilde{\sigma}_i] = \text{prox}_{\lambda\|\cdot\|_{1-2}}(\boldsymbol{\sigma}(\mathbf{Z}))$  in (6). Then, (i)  $\sigma_i(\mathbf{Z}) \geq \tilde{\sigma}_i$  (shrinkage); and (ii)  $\sigma_i(\mathbf{Z}) - \tilde{\sigma}_i \leq \sigma_{i+1}(\mathbf{Z}) - \tilde{\sigma}_{i+1}$  (adaptivity), where strict inequality holds at least for one  $i$ .*

The above properties are important for obtaining good empirical performance [13, 17]. The following Corollary shows that they are shared by the nonconvex low-rank regularizers of the form in (3).

<sup>2</sup>An affine transform  $\mathcal{A}$  satisfies the RIP [7] if for all  $\mathbf{X}$  of rank at most  $k$ , there exists a isometry constant  $\delta_k \in (0, 1)$  such that  $(1 - \delta_k)\|\mathbf{X}\|_F^2 \leq \|\mathcal{A}(\mathbf{X})\|_2^2 \leq (1 + \delta_k)\|\mathbf{X}\|_F^2$ .

**Corollary 3.4.** *The two properties in Proposition 3.3 also hold for the proximal operators of the other nonconvex low-rank regularizers of the form in (3).*

However, it is unclear if these properties also hold for  $\ell_{t,1-2}$  in general (where  $t \neq 0$ ), as the corresponding proximal operator does not have an analytic expression.

### 3.2 Solving the Low-Rank Matrix Learning Problem with NNFN Regularization

With the simple proximal operator obtained in Proposition 3.2, learning with the NNFN regularizer can be readily solved with the proximal algorithm. In Section 3.2.1, we first introduce a direct implementation based on Proposition 3.2, which still relies on computing the SVD in each iteration. In Section 3.2.2, we present a simple and efficient algorithm that avoids SVD computations by using a factorized matrix decomposition.

---

#### Algorithm 1 NNFN(naive).

---

**Input:** Randomly initialized  $\mathbf{X}^0$ , stepsize  $\eta$ ;  
1: **for**  $t = 1, \dots, T$  **do**  
2:   obtain  $\mathbf{Z}^t = \mathbf{X}^{t-1} - \eta \nabla f(\mathbf{X}^{t-1})$ ;  
3:   update  $\mathbf{X}^t$  as  $\text{prox}_{\lambda \tau_{\text{NNFN}}}(\mathbf{Z}^t)$ ;  
4: **end for**  
5: **return**  $\mathbf{X}^T$ .

---



---

#### Algorithm 2 NNFN(factored).

---

**Input:** Randomly initialized  $\mathbf{W}^0, \mathbf{H}^0$ , stepsize  $\eta$ ;  
1: **for**  $t = 1, \dots, T$  **do**  
2:   update  $\mathbf{W}^t = \mathbf{W}^{t-1} - \eta \nabla_{\mathbf{W}} F(\mathbf{W}^t, \mathbf{H}^t)$ ;  
3:   update  $\mathbf{H}^t = \mathbf{H}^{t-1} - \eta \nabla_{\mathbf{H}} F(\mathbf{W}^t, \mathbf{H}^t)$ ;  
4: **end for**  
5: **return**  $\mathbf{X}^T = \mathbf{W}^T (\mathbf{H}^T)^\top$ .

---

#### 3.2.1 Naive Solver by Proximal Algorithm

We first present a direct application of the proximal algorithm to problem (1) with the NNFN regularizer. At the  $t$ th iteration, we obtain  $\mathbf{Z}^t = \mathbf{X}^{t-1} - \eta \nabla f(\mathbf{X}^{t-1})$ , and then perform the proximal step in Proposition 3.2. The complete procedure, denoted NNFN(naive), is shown in Algorithm 1.

In the following, we study its complexities. For concreteness, we consider the context of matrix completion [6], which tries to fill in the missing entries of an incomplete matrix  $\mathbf{O} \in \mathbb{R}^{m \times n}$ . We use the square loss  $f(\mathbf{X}) = \frac{1}{2} \|\mathcal{P}_{\Omega}(\mathbf{X} - \mathbf{O})\|_F^2$ , where  $\Omega \in \{0, 1\}^{m \times n}$  is the set denoting positions of the observed entries (with  $\Omega_{ij} = 1$  if  $O_{ij}$  is observed, and 0 otherwise), and  $\mathcal{P}_{\Omega}(\cdot)$  is the projection operator such that  $[\mathcal{P}_{\Omega}(\mathbf{A})]_{ij} = A_{ij}$  if  $\Omega_{ij} = 1$  and 0 otherwise. As can be easily seen, the iteration time complexity of NNFN(naive) is dominated by SVD. Let  $r_t$  (with  $n \geq r_t \geq k$ ) be the rank estimated at the  $t$ th iteration. We perform rank- $k$  truncated SVD, which reduces the time complexity from  $O(mn^2)$  to  $O(mnk)$ . Its space complexity is  $O(mn)$ , as the complete matrix  $\mathbf{X}$  has to be kept.

#### 3.2.2 Efficient Solver by Using the Factorized Form

In this section, we propose a more efficient solver which removes the SVD bottleneck. The key observation is that the NNFN regularizer in (5) can be computed from the nuclear and Frobenius norms. Obviously, the Frobenius norm of a matrix can be computed without using its singular values. As for the nuclear norm, the following Proposition shows that it can also be rewritten in a form that does not require accessing the singular values. Thus, SVD can be completely avoided. In contrast, the other nonconvex low-rank regularizers (including the very related truncated  $\ell_{1-2}$  regularizer with  $t \neq 0$ ) need to penalize individual singular values, and so cannot utilize this factorized form.

**Lemma 3.5** ([28]). *For a matrix  $\mathbf{X}$  with rank  $k^* \leq k$ ,  $\|\mathbf{X}\|_* = \min_{\mathbf{X}=\mathbf{W}\mathbf{H}^\top} \frac{1}{2}(\|\mathbf{W}\|_F^2 + \|\mathbf{H}\|_F^2)$ , where  $\mathbf{W} \in \mathbb{R}^{m \times k}$  and  $\mathbf{H} \in \mathbb{R}^{n \times k}$ .*

This motivates us to factorize  $\mathbf{X}$  as  $\mathbf{W}\mathbf{H}^\top$ , with  $\mathbf{W} \in \mathbb{R}^{m \times k}$  and  $\mathbf{H} \in \mathbb{R}^{n \times k}$ , where  $k$  is greater than or equal to the desired rank  $k^*$  of the matrix solution. As  $k^*$  is usually unknown in practice, this  $k$  is treated as a hyperparameter. The matrix learning problem then becomes:

$$\min_{\mathbf{W}, \mathbf{H}} F(\mathbf{W}, \mathbf{H}) \equiv f(\mathbf{W}\mathbf{H}^\top) + \frac{\lambda}{2}(\|\mathbf{W}\|_F^2 + \|\mathbf{H}\|_F^2) - \lambda \|\mathbf{W}\mathbf{H}^\top\|_F. \quad (7)$$

The following Theorem shows that reformulating the optimization problem with this factorized form does not affect the recovery bound. In particular, as in Proposition 3.1, the recovery error still depends linearly on the norm of the error.



**Theorem 3.6.** With  $f(\mathbf{X}) = \frac{1}{2}\|\mathcal{A}(\mathbf{X}) - \mathbf{b}\|_2^2$ , where  $\mathcal{A}$  is an affine transform satisfying the RIP, and  $\mathbf{b} = \mathcal{A}(\mathbf{X}^*) + \mathbf{e}$  is a measurement vector corresponding to a rank- $k^*$  matrix  $\mathbf{X}^*$  and error vector  $\mathbf{e}$ . Assume that the isometry constant of  $\mathcal{A}$  satisfies  $\delta_{2k^*} \leq 1/3$ . Consider the equivalent constrained formulation of (7):  $\arg \min_{\mathbf{W}, \mathbf{H}} f(\mathbf{W}\mathbf{H}^\top)$  s.t.  $\frac{1}{2}(\|\mathbf{W}\|_F^2 + \|\mathbf{H}\|_F^2) - \|\mathbf{W}\mathbf{H}^\top\|_F \leq \beta'$ , where  $\beta' \geq 0$  is a hyperparameter. Let  $\mathbf{X}^t = \mathbf{W}^t(\mathbf{H}^t)^\top$  and assume that the sequence  $\{\mathbf{X}^t\}$  satisfying  $f(\mathbf{X}^{t+1}) < f(\mathbf{X}^t)$ . Then,  $\|\mathbf{X}^t - \mathbf{X}^*\|_F \leq c'\|\mathbf{e}\|_2$  for some constant  $c'$  and sufficiently large  $t$ .

As mentioned earlier, the main advantage of this reformulation is that problem (7) can now be directly solved by gradient descent. In particular, gradients of  $F(\mathbf{W}, \mathbf{H})$  can be easily obtained. Let  $\mathbf{Q} \equiv \mathbf{W}\mathbf{H}^\top \neq \mathbf{0}$ , and  $c = \lambda/\|\mathbf{W}\mathbf{H}^\top\|_F$ . Then,  $\nabla_{\mathbf{W}}F(\mathbf{W}, \mathbf{H}) = [\nabla_{\mathbf{Q}}f(\mathbf{Q})]\mathbf{H} + \lambda\mathbf{W} - c\mathbf{W}(\mathbf{H}^\top\mathbf{H})$ , and  $\nabla_{\mathbf{H}}F(\mathbf{W}, \mathbf{H}) = [\nabla_{\mathbf{Q}}f(\mathbf{Q})]^\top\mathbf{W} + \lambda\mathbf{H} - c\mathbf{H}(\mathbf{W}^\top\mathbf{W})$ . These only involve simple matrix multiplications, without any SVD computation.

The following guarantees its convergence to a critical point of (7), which can be used to form a critical point of the original low-rank matrix learning problem in (1).

**Theorem 3.7.** Assume that  $\mathbf{W}^t(\mathbf{H}^t)^\top \neq \mathbf{0}$  during the iterations, gradient descent on (7) can converge to a critical point  $(\bar{\mathbf{W}}, \bar{\mathbf{H}})$ . Moreover, the obtained  $\bar{\mathbf{X}} = \bar{\mathbf{W}}\bar{\mathbf{H}}^\top$  is also a critical point of (1), with  $r$  being the NNFN regularizer.

The complete procedure, which will be denoted NNFN(factored), is shown in Algorithm 2. As NNFN(factored) does not need to compute the expensive SVD, it has a much lower time complexity. Specifically, again in the context of matrix completion, multiplication of the sparse matrix  $\nabla_{\mathbf{Q}}f(\mathbf{Q}) = \mathcal{P}_{\Omega}(\mathbf{Q} - \mathbf{O})$  and  $\mathbf{H}$  in  $\nabla_{\mathbf{W}}F(\mathbf{W}, \mathbf{H})$  (and similarly multiplication of  $[\nabla_{\mathbf{Q}}f(\mathbf{Q})]^\top$  and  $\mathbf{W}$  in  $\nabla_{\mathbf{H}}F(\mathbf{W}, \mathbf{H})$ ) takes  $O(\|\Omega\|_0 k)$  time, computation of  $\mathbf{W}(\mathbf{H}^\top\mathbf{H})$ ,  $\mathbf{H}(\mathbf{W}^\top\mathbf{W})$  and  $\|\mathbf{W}\mathbf{H}^\top\|_F$  (computed as  $\sqrt{\text{tr}((\mathbf{H}^\top\mathbf{H})(\mathbf{W}^\top\mathbf{W}))}$ ) takes  $O((m+n)k^2)$  time. Thus, the iteration time complexity is  $O(\|\Omega\|_0 k + (m+n)k^2)$ . As for space, using the factorized form reduces the parameter size from  $O(mn + \|\Omega\|_0)$  to  $O(m+n)k + \|\Omega\|_0$ , where  $\|\Omega\|_0$  is the space for keeping the sparse matrix  $\mathbf{O}$ .

A comparison of the complexities with various state-of-the-art matrix completion methods that will be compared in Section 4 is shown in Table 1. As can be seen, NNFN(factored) and LMaFit have the smallest time complexities. As for space, only DCA [22] and NNFN(naive) require keeping the complete matrix which takes  $O(mn)$  space, while the other methods have comparable and much smaller space requirements.

Table 1: Comparison of the various state-of-the-art matrix completion methods that will be compared in Section 4. Here,  $r_t$  (usually  $\geq k$ ) is an estimated rank at the  $t$ th iteration,  $\hat{r}_t = r_t + r_{t-1}$ , and  $q$  is number of inner ADMM iterations used in [22].

regularizer	solver	iteration time complexity	space complexity
fixed rank [28]	LMaFit [29]	$O(\ \Omega\ _0 k + (m+n)k^2)$	$O((m+n)k + \ \Omega\ _0)$
probabilistic fixed rank [23]	BPMF [27]	$O(\ \Omega\ _0 k^2 + (m+n)k^3)$	$O((m+n)k + \ \Omega\ _0)$
nuclear norm [6]	softImpute [15]	$O(\ \Omega\ _0 k + (m+n)\hat{r}_t^2)$	$O((m+n)k + \ \Omega\ _0)$
nonconvex regularizers in (3)	FaNCL [33]	$O(\ \Omega\ _0 r_t + (m+n)\hat{r}_t^2)$	$O((m+n)r_t + \ \Omega\ _0)$
truncated $\ell_{1-2}$ [22]	DCA [22]	$O(qmn^2)$	$O(mn)$
NNFN	naive	$O(mnr_t)$	$O(mn)$
	factored	$O(\ \Omega\ _0 k + (m+n)k^2)$	$O((m+n)k + \ \Omega\ _0)$

## 4 Experiments

In this section, we perform matrix completion experiments on a number of synthetic and real-world data sets, using a PC with Intel i7 3.6GHz CPU and 48GB memory. Experiments are repeated five times, and the averaged performance reported. Because of the lack of space, results on the standard deviation of the performance are shown in Appendix B.2.

### 4.1 Setup

The proposed method NNFN(factored), which is based on the factorized matrix form, and its slower variant NNFN(naive), which is based on the direct application of proximal algorithm, will

be compared with both low-rank regularization and matrix factorization algorithms. The low-rank regularizers compared include: (i) convex nuclear norm regularizer  $\|\mathbf{X}\|_*$  [6, 31], optimized by the recent softImpute algorithm via alternating least squares [15]; (ii) nonconvex low-rank regularizers of the form (3), including the capped- $\ell_1$  penalty [35], log-sum penalty (LSP) [8]; and minimax concave penalty (MCP) [34], optimized by the low-rank matrix learning solver FaNCL [33]; and (iii) truncated  $\ell_{1-2}$  regularizer in (4) [22], which is optimized with DCA algorithm with sub-problems solved by ADMM. As for the matrix factorization algorithms, these include: (i) low-rank matrix fitting algorithm (LMaFit) [29], which solves  $\min_{\mathbf{W}, \mathbf{H}} f(\mathbf{W}\mathbf{H}^\top) + \frac{\lambda}{2}(\|\mathbf{W}\|_F^2 + \|\mathbf{H}\|_F^2)$ ; and (ii) Bayesian probabilistic matrix factorization (BPMF) [23], which is a Bayesian model trained with Markov chain Monte Carlo [12]. All the algorithms are implemented in MATLAB (with sparse tensor and matrix operations written in C as MEX functions) and obtained from the respective authors. Each algorithm is stopped when the relative difference between objective values in consecutive iterations is smaller than  $10^{-4}$ . All hyperparameters including  $\lambda$ ,  $k$ , hyperparameters required by compared methods and stepsize are tuned by grid search using the validation set. More details are in Appendix B.1.

**Evaluation Metrics.** Given a partially observed matrix  $\mathbf{O}$ , let  $\Omega^\perp$  be the matrix indexing positions of the unobserved elements (i.e.,  $\Omega_{ij}^\perp = 0$  if  $O_{ij}$  is observed, and 1 otherwise), and  $\bar{\mathbf{X}}$  be the matrix recovered. Following [26, 33, 32], performance on the synthetic data is measured by the normalized mean squared error (NMSE) on  $\Omega^\perp$ :  $\text{NMSE} = \|P_{\Omega^\perp}(\bar{\mathbf{X}} - \mathbf{G})\|_F / \|P_{\Omega^\perp}(\mathbf{G})\|_F$ , where  $\mathbf{G}$  is the ground-truth matrix. On the real-world data sets, we use the root mean squared error (RMSE) on  $\Omega^\perp$ :  $\text{RMSE} = \sqrt{\|P_{\Omega^\perp}(\bar{\mathbf{X}} - \mathbf{O})\|_F^2 / \|\Omega^\perp\|_0}$ . Besides the error, we also report the training time in seconds. Due to the lack of space, rank of the recovered matrix is reported in Appendix B.2.

## 4.2 Synthetic Data

First,  $\mathbf{W}, \mathbf{H} \in \mathbb{R}^{m \times k^*}$  are generated with elements sampled i.i.d. from the standard normal distribution  $\mathcal{N}(0, 1)$ . We set  $k^* = 5$ , and vary  $m$  in  $\{500, 1000, 2000\}$ . The  $m \times m$  ground-truth matrix (with rank  $k^*$ ) is then constructed as  $\mathbf{G} = \mathbf{W}\mathbf{H}^\top$ . The observed matrix  $\mathbf{O}$  is generated by adding noise matrix  $\mathbf{E}$  to  $\mathbf{G}$ :  $\mathbf{O} = \mathbf{G} + \mathbf{E}$ . The elements of  $\mathbf{E}$  are sampled from  $\mathcal{N}(0, 0.1)$ . A set of  $\|\Omega\|_0 = 2mk^* \log(m)$  random elements in  $\mathbf{O}$  are observed. 50% of them are randomly sampled for training, and the rest is taken as validation set for hyperparameter tuning. We define the sparsity ratio  $s$  of the observed matrix as its fraction of observed elements (i.e.,  $s = \|\Omega\|_0 / m^2$ ).

Table 2 shows the results. As can be seen, nonconvex regularizers (including the proposed  $r_{\text{NNFN}}$ ) consistently yield better recovery performance. Among the nonconvex regularizers, all of them yield comparable errors. As for the rank (reported in Appendix B.2), all methods (except the nuclear norm regularizer) can recover the true rank. As for speed, NNFN(factored) allows significantly faster optimization than NNFN(naive), which validates the efficiency of using the factorized form. LMaFit and BPMF, though also using a factorized form, are much slower. This is because LMaFit uses the QR decomposition to solve the least squares subproblem, which is slow in practice, while BPMF uses expensive Markov chain Monte Carlo in inference. NNFN(factored) is orders of magnitude faster than the other methods. Optimization with the truncated  $\ell_{1-2}$  is exceptionally slow, which is due to the need of having two levels of DCA and ADMM iterations. Figure 1 shows convergence of the testing NMSE with (training) clock time. As can be seen, NNFN(factored) always has the fastest convergence to the lowest NMSE.

**Effects of Noise, Rank and Sparsity Ratio.** In this section, we vary (i) the variance of the Gaussian noise matrix  $\mathbf{E}$  in the range  $\{0.01, 0.1, 1\}$ ; (ii) the true rank  $k^*$  of the data in  $\{5, 10, 20\}$ ; and (iii) the sparsity ratio  $s$  in  $\{0.5, 1, 2\} \times (2mk^* \log(m) / m^2)$ . The experiment is performed on the synthetic data set, with  $m = 1000$ . In each trial, we only vary one variable while keeping the others at default ( $k^* = 5$ ,  $\mathbf{E} \sim \mathcal{N}(0, 0.1)$  and  $s = 6.91\%$ ). Figure 2 shows the testing NMSE results. As expected, a larger noise, smaller true rank, or sparser matrix lead to a harder matrix completion problem and subsequently higher NMSE's. However, the relative performance ranking of the various methods remain the same, and nonconvex regularization always obtain the best NMSE. Different settings do not affect the relative time results (results are in Appendix B.2). NNFN(factored) is consistently faster than the others.

Table 2: Performance on the synthetic data with different dimensionalities ( $m$ 's). For each data set, its sparsity ratio is shown in brackets. Error is the testing NMSE scaled by  $10^{-2}$ . The best and comparable results (according to the pairwise t-test with 95% confidence) are highlighted in bold.

	$m = 500$ (12.43%)		$m = 1000$ (6.91%)		$m = 2000$ (3.80%)	
	error	time (s)	error	time (s)	error	time (s)
LMaFit	2.46	0.08	2.18	0.3	1.98	1.5
BPMF	2.34	3.2	2.03	5.8	1.88	48.3
nuclear norm	4.36	2.1	3.75	4.2	3.33	40.9
capped- $\ell_1$	<b>1.97</b>	0.8	<b>1.83</b>	5.4	<b>1.78</b>	36.0
LSP	<b>1.97</b>	0.8	<b>1.83</b>	5.1	<b>1.77</b>	35.1
MCP	<b>1.96</b>	0.7	<b>1.82</b>	4.1	<b>1.78</b>	40.6
truncated $\ell_{1-2}$	<b>1.96</b>	695.8	<b>1.82</b>	1083.2	<b>1.77</b>	3954.1
NNFN(naive)	<b>1.96</b>	2.1	<b>1.82</b>	7.7	<b>1.77</b>	43.1
NNFN(factored)	<b>1.96</b>	<b>0.04</b>	<b>1.82</b>	<b>0.08</b>	<b>1.77</b>	<b>0.3</b>

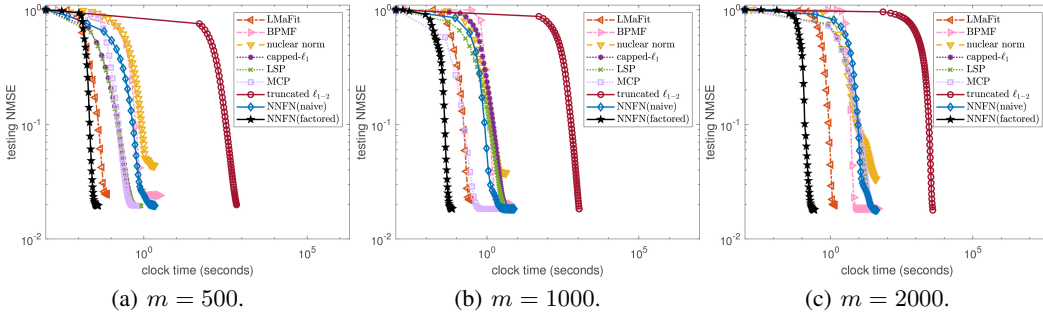


Figure 1: Testing NMSE versus clock time on the synthetic data sets.

### 4.3 Real-World Data

In this section, experiments are performed on three kinds of popular benchmark data sets (details reported in Appendix B.1): (i) recommendation data [19]; (ii) hyperspectral images [33]; and (iii) climate data [1].

**Recommendation Data.** The popular *MovieLens* (of size  $6,040 \times 3,449$ ) and *Yahoo* data sets (of size  $249,012 \times 296,111$ )[19] are used. We uniformly sample 50% of the ratings as observed for training, 25% for validation (hyperparameter tuning) and the rest for testing. Figure 3 shows convergence of the testing RMSE. Again, NNFN(factored) converges much faster than the other methods to a lower testing RMSE (which is consistent with recovery performance and timing results reported in Appendix B.2). Optimization with the nuclear norm, truncated  $\ell_{1-2}$  and NNFN(naive) cannot converge in three hours on *Yahoo*, and thus are not reported.

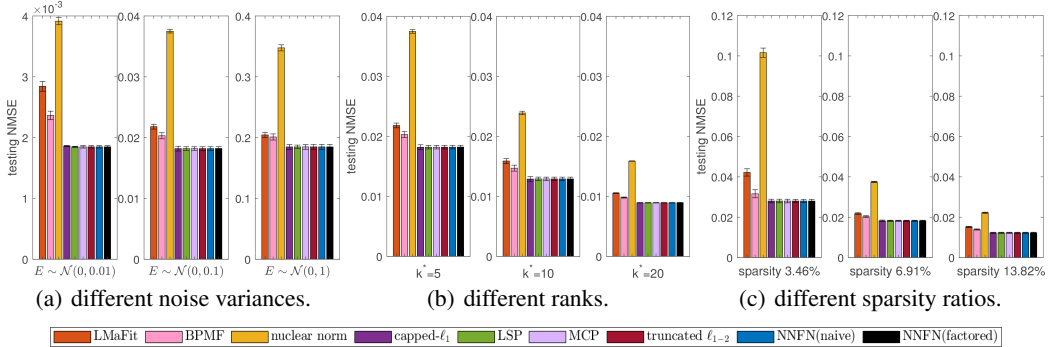


Figure 2: Testing NMSE with different settings on synthetic data ( $m = 1000$ ).

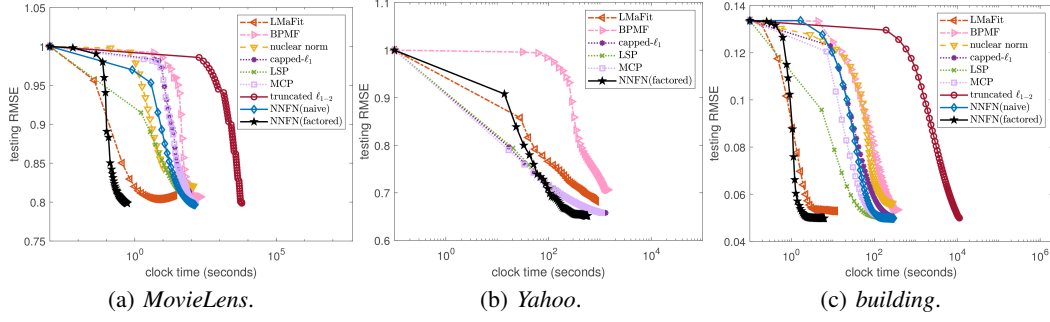


Figure 3: Testing RMSE versus clock time on the recommendation (Figure 3(a) and 3(b)) and hyperspectral (Figure 3(c)) data. Result for *cabbage* is similar and is shown in Appendix B.2.

**Hyperspectral Data.** Hyperspectral images of *building* (reshaped to  $1, 258, 208 \times 49$ ) and *cabbage* (reshaped to  $692, 736 \times 49$ ) from [33] are used. The task is to fill in the missing pixels. The pixels are normalized to zero mean and unit variance, and noise from  $\mathcal{N}(0, 0.01)$  added. We randomly sample 5% of the pixels for training, 5% for validation and the rest for testing. Figure 3 shows convergence of the testing RMSE. As can be seen, nonconvex regularizers obtain the best recovery performance than the other methods. In terms of speed, NNFN(factored) is again the fastest. Similar observations on recovery error and timing results (reported in Appendix B.2) show that only NNFN(factored) is both efficient and effective.

**Climate Data.** The *GAS* and *USHCN* data sets from [1] are used. *GAS* contains monthly observations for the green gas components, of which we use  $CO_2$  and  $H_2$ . *USHCN* contains monthly temperature and precipitation readings. More details about the data are in Appendix B.1. The task is to predict climate observations for locations that do not have any records. Following [1], we normalize the data to zero mean and unit variance, then randomly sample 10% of the locations for training, another 10% for validation, and the rest for testing. Results are shown in Table 3. They are consistent with the observations in the previous experiments. In terms of recovery performance, all the nonconvex regularizers (including NNFN(naive) and NNFN(factored)) have comparable performance and obtain the lowest testing RMSE. In terms of speed, NNFN(factored) is again the fastest, and its speed advantage is particularly apparent on the larger *USHCN* data set. Convergence of the RMSE (reported in Appendix B.2) shows that NNFN(factored) again shows the fastest convergence to the lowest testing RMSE.

Table 3: Performance on the climate data sets. Error is RMSE scaled by  $10^{-1}$ . The best and comparable results (according to the pairwise t-test with 95% confidence) are highlighted in bold.

	<i>GAS</i>				<i>USHCN</i>			
	$CO_2$		$H_2$		temperature		precipitation	
	error	time(s)	error	time(s)	error	time(s)	error	time(s)
LMaFit	5.65	0.17	5.74	0.19	4.83	15.7	8.23	33.3
BPMF	5.52	3.2	5.54	3.4	4.64	148.1	8.19	125.1
GRALS	5.83	0.7	5.78	0.4	4.98	37.2	8.25	49.6
nuclear norm	5.84	1.0	5.93	0.8	4.80	108.5	8.28	84.9
capped- $\ell_1$	5.33	0.6	<b>5.31</b>	0.7	4.50	108.5	<b>8.06</b>	87.2
LSP	5.37	1.2	5.40	1.3	4.48	133.3	<b>8.06</b>	105.8
MCP	<b>5.30</b>	1.0	5.34	0.5	<b>4.44</b>	92.5	<b>8.06</b>	85.2
truncated $\ell_{1-2}$	<b>5.30</b>	11.0	<b>5.31</b>	7.3	<b>4.44</b>	573.9	<b>8.06</b>	318.5
NNFN(naive)	<b>5.30</b>	0.4	<b>5.31</b>	0.5	<b>4.44</b>	57.1	<b>8.06</b>	66.4
NNFN(factored)	<b>5.30</b>	<b>0.05</b>	<b>5.31</b>	<b>0.05</b>	<b>4.44</b>	<b>5.9</b>	<b>8.06</b>	<b>13.5</b>

## 5 Conclusion

Learning with existing nonconvex low-rank regularizers offers good recovery performance but is slow, due to the need to compute SVD in each iteration. In this paper, we proposed a novel nonconvex

low-rank regularizer with proved adaptive shrinkage. Unlike existing nonconvex regularizers which requires access to individual singular value, this regularizer can be formulated into a factored matrix form which bypasses the computation of the expensive SVD. We show that learning with this factorized form guarantees stable recovery and can be optimized by any gradient-based method with convergence guarantee. Extensive experiments show that the proposed algorithm achieves state-of-the-art recovery performance comparable with the existing nonconvex low-rank regularizers, but is much more efficient than existing low-rank convex / nonconvex regularization and matrix factorization algorithms.

## References

- [1] M. T. Bahadori, Q. R. Yu, and Y. Liu. Fast multivariate spatio-temporal analysis via low rank tensor learning. In *Advances in Neural Information Processing Systems*, pages 3491–3499, 2014.
- [2] S. Boyd, N. Parikh, E. Chu, B. Peleato, and J. Eckstein. Distributed optimization and statistical learning via the alternating direction method of multipliers. *Foundations and Trends in Machine Learning*, 3(1):1–122, 2011.
- [3] S. P. Boyd and L. Vandenberghe. *Convex Optimization*. Cambridge University Press, 2004.
- [4] J.-F. Cai, E. J. Candès, and Z. Shen. A singular value thresholding algorithm for matrix completion. *SIAM Journal on Optimization*, 20(4):1956–1982, 2010.
- [5] E. J. Candès, X. Li, Y. Ma, and J. Wright. Robust principal component analysis? *Journal of the ACM*, 58(3):1–37, 2011.
- [6] E. J. Candès and B. Recht. Exact matrix completion via convex optimization. *Foundations of Computational Mathematics*, 9(6):717–772, 2009.
- [7] E. J. Candes and T. Tao. Decoding by linear programming. *IEEE Transactions on Information Theory*, 51(12):4203–4215, 2005.
- [8] E. J. Candes, M. B. Wakin, and S. P. Boyd. Enhancing sparsity by reweighted  $\ell_1$  minimization. *Journal of Fourier Analysis and Applications*, 14(5-6):877–905, 2008.
- [9] J. Chen, J. Zhou, and J. Ye. Integrating low-rank and group-sparse structures for robust multi-task learning. In *International Conference on Knowledge Discovery and Data Mining*, pages 42–50, 2011.
- [10] D. L. Donoho, I. M. Johnstone, G. Kerkycharian, and D. Picard. Wavelet shrinkage: Asymptopia? *Journal of the Royal Statistical Society: Series B*, 57(2):301–337, 1995.
- [11] M. Fazel. *Matrix Rank Minimization with Applications*. PhD thesis, Stanford, 2002.
- [12] W. R. Gilks, S. Richardson, and D. Spiegelhalter. *Markov Chain Monte Carlo in Practice*. CRC Press, 1995.
- [13] S. Gu, L. Zhang, W. Zuo, and X. Feng. Weighted nuclear norm minimization with application to image denoising. In *Conference on Computer Vision and Pattern Recognition*, pages 2862–2869, 2014.
- [14] H. Gui, J. Han, and Q. Gu. Towards faster rates and oracle property for low-rank matrix estimation. In *International Conference on Machine Learning*, pages 2300–2309, 2016.
- [15] T. Hastie, R. Mazumder, J. D. Lee, and R. Zadeh. Matrix completion and low-rank svd via fast alternating least squares. *Journal of Machine Learning Research*, 16(1):3367–3402, 2015.
- [16] J.-B. Hiriart-Urruty. Generalized differentiability, duality and optimization for problems dealing with differences of convex functions. In *Proceedings of the Symposium on Convexity and Duality in Optimization*, pages 37–70, 1985.
- [17] Y. Hu, D. Zhang, J. Ye, X. Li, and X. He. Fast and accurate matrix completion via truncated nuclear norm regularization. *IEEE Transactions on Pattern Analysis and Machine Intelligence*, 35(9):2117–2130, 2012.
- [18] A. Jennings and J. McKeown. *Matrix Computation*. John Wiley & Sons, 1992.
- [19] Y. Koren, R. Bell, and C. Volinsky. Matrix factorization techniques for recommender systems. *Computer*, 42(8):30–37, 2009.

- [20] G. Liu, Z. Lin, S. Yan, J. Sun, Y. Yu, and Y. Ma. Robust recovery of subspace structures by low-rank representation. *IEEE Transactions on Pattern Analysis and Machine Intelligence*, 35(1):171–184, 2012.
- [21] C. Lu, C. Zhu, C. Xu, S. Yan, and Z. Lin. Generalized singular value thresholding. In *AAAI Conference on Artificial Intelligence*, pages 1805–1811, 2015.
- [22] T.-H. Ma, Y. Lou, and T.-Z. Huang. Truncated  $\ell_{1-2}$  models for sparse recovery and rank minimization. *SIAM Journal on Imaging Sciences*, 10(3):1346–1380, 2017.
- [23] A. Mnih and R. R. S. Probabilistic matrix factorization. In *Advances in Neural Information Processing Systems*, pages 1257–1264, 2008.
- [24] J. Nocedal and S. Wright. *Numerical Optimization*. Springer Science & Business Media, 2006.
- [25] N. Parikh and S. Boyd. Proximal algorithms. *Foundations and Trends in Optimization*, 1(3):127–239, 2014.
- [26] N. Rao, H.-F. Yu, P. K. Ravikumar, and I. S. Dhillon. Collaborative filtering with graph information: Consistency and scalable methods. In *Advances in Neural Information Processing Systems*, pages 2107–2115, 2015.
- [27] R. Salakhutdinov and A. Mnih. Bayesian probabilistic matrix factorization using markov chain monte carlo. In *International Conference on Machine Learning*, pages 880–887, 2008.
- [28] N. Srebro, J. Rennie, and T. S. Jaakkola. Maximum-margin matrix factorization. In *Advances in Neural Information Processing Systems*, pages 1329–1336, 2005.
- [29] Z. Wen, W. Yin, and Y. Zhang. Solving a low-rank factorization model for matrix completion by a nonlinear successive over-relaxation algorithm. *Mathematical Programming Computation*, 4(4):333–361, 2012.
- [30] Q. Yao and J. T. Kwok. Efficient learning with a family of nonconvex regularizers by redistributing nonconvexity. *Journal of Machine Learning Research*, 18(1):6574–6625, 2017.
- [31] Q. Yao and J. T. Kwok. Accelerated and inexact soft-impute for large-scale matrix and tensor completion. *IEEE Transactions on Knowledge and Data Engineering*, 31(9):1665–1679, 2018.
- [32] Q. Yao, J. T. Kwok, F. Gao, W. Chen, and T.-Y. Liu. Efficient inexact proximal gradient algorithm for nonconvex problems. In *International Joint Conference on Artificial Intelligence*, pages 3308–3314, 2017.
- [33] Q. Yao, J. T. Kwok, T. Wang, and T.-Y. Liu. Large-scale low-rank matrix learning with nonconvex regularizers. *IEEE Transactions on Pattern Analysis and Machine Intelligence*, 41(11):2628–2643, 2019.
- [34] C.-H. Zhang. Nearly unbiased variable selection under minimax concave penalty. *The Annals of Statistics*, 38(2):894–942, 2010.
- [35] T. Zhang. Analysis of multi-stage convex relaxation for sparse regularization. *Journal of Machine Learning Research*, 11(Mar):1081–1107, 2010.

## A Proof

### A.1 Proposition 3.2

*Proof.* Let  $\mathbf{X} = \mathbf{U}\text{Diag}(\tilde{\boldsymbol{\sigma}})\mathbf{V}^\top$  and  $\mathbf{Z} = \bar{\mathbf{U}}\text{Diag}(\boldsymbol{\sigma}(\mathbf{Z}))\bar{\mathbf{V}}^\top$  be the SVD decomposition of  $\mathbf{X}$  and  $\mathbf{Z}$ . By simple expansion, we have

$$\begin{aligned} & \frac{1}{2}\|\mathbf{X} - \mathbf{Z}\|_F^2 + \lambda r_{\text{NNFN}}(\mathbf{X}) \\ &= \frac{1}{2}\text{tr}(\mathbf{X}^\top \mathbf{X} + \mathbf{Z}^\top \mathbf{Z} - 2\mathbf{X}^\top \mathbf{Z}) + \lambda(\|\mathbf{X}\|_* - \theta\|\mathbf{X}\|_F) \\ &= \frac{1}{2}(\|\tilde{\boldsymbol{\sigma}}\|_2^2 + \|\boldsymbol{\sigma}(\mathbf{Z})\|_2^2) - \text{tr}(\mathbf{X}^\top \mathbf{Z}) + \lambda\|\tilde{\boldsymbol{\sigma}}\|_1 - \lambda\theta\|\tilde{\boldsymbol{\sigma}}\|_2. \end{aligned}$$

Recall that  $\text{tr}(\mathbf{X}^\top \mathbf{Z}) \leq \tilde{\boldsymbol{\sigma}}^\top \boldsymbol{\sigma}(\mathbf{Z})$  achieves its equality at  $\mathbf{U} = \bar{\mathbf{U}}, \mathbf{V} = \bar{\mathbf{V}}$  [18]. Then solving (6) can be instead computed by solving  $\tilde{\boldsymbol{\sigma}}$  as

$$\begin{aligned} & \arg \min_{\tilde{\boldsymbol{\sigma}}} \frac{1}{2}\|\tilde{\boldsymbol{\sigma}} - \boldsymbol{\sigma}(\mathbf{Z})\|_2^2 + \lambda(\|\tilde{\boldsymbol{\sigma}}\|_1 - \theta\|\tilde{\boldsymbol{\sigma}}\|_2) \\ & \text{s.t. } \tilde{\sigma}_1 \geq \tilde{\sigma}_2 \geq \dots \geq \tilde{\sigma}_m \geq 0. \end{aligned} \quad (8)$$

It can be solved by proximal operator as  $\tilde{\boldsymbol{\sigma}} = \text{prox}_{\lambda\|\cdot\|_{1-2}}(\boldsymbol{\sigma}(\mathbf{Z}))$ . The constraint in (8) is naturally satisfied. As  $\sigma_i(\mathbf{Z}) \geq 0$  and  $\sigma_i(\mathbf{Z}) \geq \sigma_{i+1}(\mathbf{Z}) \forall i$ , we must have  $\tilde{\sigma}_i \geq 0$  and  $\tilde{\sigma}_i \geq \tilde{\sigma}_{i+1} \forall i$ . Otherwise, we can always swap the sign or value of  $\tilde{\sigma}_i$  and  $\tilde{\sigma}_{i+1}$  and obtain a smaller objective of (8).  $\square$

### A.2 Proposition 3.3

*Proof.* Let  $\mathbf{X} = \mathbf{U}\text{Diag}(\tilde{\boldsymbol{\sigma}})\mathbf{V}^\top$  where  $\tilde{\boldsymbol{\sigma}} = \text{prox}_{\lambda\|\cdot\|_{1-2}}(\boldsymbol{\sigma}(\mathbf{Z}))$ . Now we prove that

- shrinkage:  $\sigma_i(\mathbf{Z}) \geq \tilde{\sigma}_i$ ,
- adaptivity:  $\sigma_i(\mathbf{Z}) - \tilde{\sigma}_i \leq \sigma_{i+1}(\mathbf{Z}) - \tilde{\sigma}_{i+1}$ , where the strict inequality holds at least for one  $i$ .

The first point: From Proposition 3.2, we can see the optimization problem on matrix (6) can be transformed to an optimization problem on singular values (8). As shown in Proposition 3.2, for  $\tilde{\boldsymbol{\sigma}} = \text{prox}_{\lambda\|\cdot\|_{1-2}}(\boldsymbol{\sigma}(\mathbf{Z}))$ , we have  $\sigma_i(\mathbf{Z}) \geq \tilde{\sigma}_i \geq 0$ .

The second point: The optimal of (8) satisfies

$$\tilde{\boldsymbol{\sigma}} - \boldsymbol{\sigma}(\mathbf{Z}) + \lambda - \lambda \frac{\tilde{\boldsymbol{\sigma}}}{\|\tilde{\boldsymbol{\sigma}}\|_2} = 0.$$

As  $\sigma_i(\mathbf{Z}) \geq \tilde{\sigma}_i \geq 0$ , we have

$$\sigma_i(\mathbf{Z}) - \tilde{\sigma}_i = \lambda - \lambda \frac{\tilde{\sigma}_i}{\|\tilde{\boldsymbol{\sigma}}\|_2} \geq 0.$$

Then as  $\tilde{\sigma}_i \geq \tilde{\sigma}_{i+1}$ , we have

$$\lambda - \lambda \frac{\tilde{\sigma}_i}{\|\tilde{\boldsymbol{\sigma}}\|_2} \leq \lambda - \lambda \frac{\tilde{\sigma}_{i+1}}{\|\tilde{\boldsymbol{\sigma}}\|_2},$$

and correspondingly  $\sigma_i(\mathbf{Z}) - \tilde{\sigma}_i \leq \sigma_{i+1}(\mathbf{Z}) - \tilde{\sigma}_{i+1}$ . The inequality holds only when  $\sigma_i(\mathbf{Z}) \neq \sigma_{i+1}(\mathbf{Z})$ .  $\square$

### A.3 Corollary 3.4

**Lemma A.1.** Let  $\hat{r}(\alpha)$  be a nonlinear, concave and non-decreasing function for  $\alpha \geq 0$  with  $\hat{r}(0) = 0$ , and

$$p = \arg \min_x \frac{1}{2}(x - z)^2 + \lambda \hat{r}(|x|). \quad (9)$$

Then, when  $z \geq 0$ , we have

- $0 \leq p \leq z$ ,
- $z_1 - p(z_1) \leq z_2 - p_2$  for  $z_1 \geq z_2$ .

*Proof.* The first point: Obvious, when  $z \geq 0$ ,  $p \geq 0$ . Next, we prove  $p \leq z$  by contradiction. Assume that  $p > z$ . Then as  $\hat{r}$  is non-decreasing, we have

$$\hat{r}(|p|) \geq \hat{r}(|z|).$$

Therefore we get

$$\frac{1}{2}(p - z)^2 + \lambda \hat{r}(|z'|) > \frac{1}{2}(z - z)^2 + \lambda \hat{r}(|z|),$$

which leads to a contradiction that  $p$  is the minimum solution found by optimizing (9). Thus,  $p \leq z$ .

The second point: The optimal of (9)  $p$  satisfies

$$p - z + \lambda \partial \hat{r}(p) = 0. \quad (10)$$

As  $\hat{r}$  is concave, for  $z_1 \geq z_2$ , we have

$$\partial \hat{r}(p_1) \leq \partial \hat{r}(p_2). \quad (11)$$

Combining (11) and (10), we get

$$z_1 - p_1 \leq z_2 - p_2,$$

and the second point is proved.  $\square$

Now, we can prove Proposition 3.3.

*Proof.* As introduced in Section 2, common nonconvex regularizers (Table 4) can be written into (3).

Table 4: Common nonconvex low-rank regularizers.

	$\hat{r}(\sigma_i(\mathbf{X}))$
capped- $\ell_1$ [35]	$\min(\sigma_i(\mathbf{X}), \theta)$
LSP [8]	$\log\left(\frac{1}{\theta}\sigma_i(\mathbf{X}) + 1\right)$
MCP [34]	$\begin{cases} \sigma_i(\mathbf{X}) - \frac{\sigma_i^2(\mathbf{X})}{2\theta\lambda} & \text{if } \sigma_i(\mathbf{X}) \leq \theta\lambda \\ \frac{\theta\lambda}{2} & \text{otherwise} \end{cases}$

Let the SVD of  $\mathbf{Z}$  be  $\bar{\mathbf{U}}\text{Diag}(\sigma(\mathbf{Z}))\bar{\mathbf{V}}^\top$ . From Theorem 1 in [21], we have

$$\tilde{\mathbf{X}} \equiv \text{prox}_{\lambda\hat{r}}(\mathbf{Z}) = \bar{\mathbf{U}}\text{Diag}(\tilde{\sigma})\bar{\mathbf{V}}^\top,$$

where  $\tilde{\sigma}_i = \text{prox}_{\lambda\hat{r}}(\sigma_i(\mathbf{Z}))$ . Then, as every singular value  $\sigma_i(\mathbf{Z})$  is nonnegative, by Lemma A.1, we get the conclusion. Note that since  $\hat{r}$  is not linear, thus the strict inequality in  $\sigma_i(\mathbf{Z}) - \tilde{\sigma}_i \leq \sigma_{i+1}(\mathbf{Z}) - \tilde{\sigma}_{i+1}$  holds at least for one  $i$ .  $\square$

#### A.4 Theorem 3.6

*Proof.* In (7), a regularized low-rank matrix learning problem is solved. This can be transformed into the following constrained problem [3, 24]:

$$\min_{\mathbf{W}, \mathbf{H}} f(\mathbf{W}\mathbf{H}^\top) \text{ s.t. } (\mathbf{W}, \mathbf{H}) \in \mathcal{C} \equiv \{(\mathbf{W}, \mathbf{H}) : \frac{1}{2}(\|\mathbf{W}\|_F^2 + \|\mathbf{H}\|_F^2) - \|\mathbf{W}\mathbf{H}^\top\|_F \leq \beta'\}, \quad (12)$$

where  $\beta' \geq 0$  is a hyperparameter. These two forms obtain equivalent solutions [3]. Therefore, we prove for the constrained problem, while the conclusion applies for both forms.

Let  $\mathbf{X}^t = \mathbf{W}^t(\mathbf{H}^t)^\top$  and assume that the sequence  $\{\mathbf{X}^t\}$  satisfying  $f(\mathbf{X}^{t+1}) \leq f(\mathbf{X}^t)$ . This sequence can be obtained by optimizing (12) via projected gradient descent which guarantees sufficient decrease in  $f$  [3, 24].



Obviously, the optimal  $\mathbf{X}^*$  satisfies  $\mathbf{b} - \mathcal{A}(\mathbf{X}^*) = \mathbf{e}$  and hence  $f(\mathbf{X}^*) = \frac{1}{2} \|\mathcal{A}(\mathbf{X}^*) - \mathbf{b}\|_2^2 = \frac{\|\mathbf{e}\|_2^2}{2}$ . Thus  $\mathbf{X}^t$  obtained at the  $t$ th iteration satisfies  $f(\mathbf{X}^t) \geq \frac{c_1^2 \|\mathbf{e}\|_2^2}{2} \geq \frac{\|\mathbf{e}\|_2^2}{2}$  for constant  $c_1$  whose absolute value is larger than 1. By choosing the dimension  $k$  of  $\mathbf{W} \in \mathbb{R}^{m \times k}$ , one can let  $\mathbf{X}^t \leq k^*$ , where  $k^*$  is the true rank of the optimal matrix  $\mathbf{X}^*$ .

We can derive

$$\begin{aligned} \|\mathcal{A}(\mathbf{X}^* - \mathbf{X}^t)\|_2^2 &\leq \|(\mathbf{b} - \mathcal{A}(\mathbf{X}^t)) - \mathbf{e}\|_2^2, \\ &\leq 2 \left( f(\mathbf{X}^t) - \mathbf{e}^\top (\mathbf{b} - \mathcal{A}(\mathbf{X}^t)) + \frac{\|\mathbf{e}\|_2^2}{2} \right), \\ &\leq 2 \left( f(\mathbf{X}^t) + \frac{2}{c_1} f(\mathbf{X}^t) + \frac{1}{c_1^2} f(\mathbf{X}^t) \right), \\ &\leq 2 \left( 1 + \frac{1}{c_1} \right)^2 f(\mathbf{X}^t) \end{aligned} \quad (13)$$

Now, we are ready to bound the difference between this  $\mathbf{X}^t$  and the optimal  $\mathbf{X}^*$ .

$$\|\mathbf{X}^t - \mathbf{X}^*\|_F^2 \leq \frac{1}{1 - \delta_{2k^*}} \|\mathcal{A}(\mathbf{X}^t - \mathbf{X}^*)\|_2^2 \quad (14)$$

$$\leq \frac{2}{1 - \delta_{2k^*}} \left( 1 + \frac{1}{c_1} \right)^2 f(\mathbf{X}^t) \quad (15)$$

$$\begin{aligned} &\leq \frac{1}{1 - \delta_{2k^*}} \left( 1 + \frac{1}{c_1} \right)^2 (c_1^2 + \epsilon) \|\mathbf{e}\|_2^2 \\ &= \frac{(c_1 + 1)^2 (c_1^2 + \epsilon) \|\mathbf{e}\|_2^2}{c_1^2 (1 - \delta_{2k^*})}, \end{aligned} \quad (16)$$

where the isometry constant is  $\delta_{2k^*}$  as  $\mathbf{X}^t - \mathbf{X}^*$  is a matrix of rank at most  $2k^*$ , (14) is derived from RIP, (15) comes from (13), and (16) is obtained as one can choose a small constant  $\epsilon$  such that  $\frac{(c_1^2 + \epsilon) \|\mathbf{e}\|_2^2}{2} \geq f(\mathbf{X}^t) \geq \frac{c_1^2 \|\mathbf{e}\|_2^2}{2}$ .

□

## A.5 Theorem 3.7

*Proof.* For smooth functions, gradient descent can obtain sufficient decrease as shown in the following Proposition.

**Proposition A.2** ([24]). *A differentiable function  $h$  with  $L$ -Lipschitz continuous gradient, i.e.,  $\|\nabla_x h(x^t) - \nabla_x h(x^{t+1})\|_2 \leq L \|x^t - x^{t+1}\|_2$ , satisfies the following inequality,*

$$h(x^t) - h(x^{t+1}) \geq \frac{1}{2L} \|\nabla_x h(x^t)\|_F^2.$$

*Moreover, when  $h$  is bounded from below, i.e.,  $\inf h(x) > -\infty$  and  $\lim_{\|x\|_2 \rightarrow \infty} h(x) = \infty$ , optimizing  $h$  by gradient descent is guaranteed to converge.*

Since  $\mathbf{W}_t \mathbf{H}_t^\top \neq \mathbf{0}$ ,  $F(\mathbf{W}, \mathbf{H})$  is smooth. As gradient descent is used, we then have

$$F(\mathbf{W}^t, \mathbf{H}^t) - F(\mathbf{W}^{t+1}, \mathbf{H}^{t+1}) \geq \frac{\eta}{2} \|\nabla_{\mathbf{W}} F(\mathbf{W}^t, \mathbf{H}^t)\|_F^2 + \frac{\eta}{2} \|\nabla_{\mathbf{H}} F(\mathbf{W}^t, \mathbf{H}^t)\|_F^2.$$

At the  $(T+1)$ th iteration, the difference between  $F(\mathbf{W}^1, \mathbf{H}^1)$  and  $F(\mathbf{W}^{T+1}, \mathbf{H}^{T+1})$  is calculated as

$$F(\mathbf{W}^1, \mathbf{H}^1) - F(\mathbf{W}^{T+1}, \mathbf{H}^{T+1}) \geq \sum_{t=1}^T \frac{\eta}{2} \|\nabla_{\mathbf{W}} F(\mathbf{W}^t, \mathbf{H}^t)\|_F^2 + \frac{\eta}{2} \|\nabla_{\mathbf{H}} F(\mathbf{W}^t, \mathbf{H}^t)\|_F^2. \quad (17)$$

As assumed,  $\lim_{\|\mathbf{W}\|_F \rightarrow \infty} F(\mathbf{W}, \cdot) = \infty$ ,  $\lim_{\|\mathbf{H}\|_F \rightarrow \infty} F(\cdot, \mathbf{H}) = \infty$ . Thus  $\infty > F(\mathbf{W}^1, \mathbf{H}^1) - F(\mathbf{W}^{T+1}, \mathbf{H}^{T+1}) \geq c$ , where  $c$  is a finite constant. Combining this with (17), when  $T \rightarrow \infty$ , we see

that a sum of infinite sequence is smaller than a finite constant. This means the sequence  $\{\mathbf{W}^t, \mathbf{H}^t\}$  has limit points. Let  $\{\bar{\mathbf{W}}, \bar{\mathbf{H}}\}$  be a limit point, we must have

$$\nabla_{\mathbf{W}} F(\bar{\mathbf{W}}, \bar{\mathbf{H}}) = 0 \text{ and } \nabla_{\mathbf{H}} F(\bar{\mathbf{W}}, \bar{\mathbf{H}}) = 0.$$

By definition, this shows  $\{\bar{\mathbf{W}}, \bar{\mathbf{H}}\}$  is a critical point of (7).

Next, we proceed to prove that  $\bar{\mathbf{X}} = \bar{\mathbf{W}}\bar{\mathbf{H}}^\top$  is the the critical point of (1) with  $r(\mathbf{X}) = r_{\text{NNFN}}(\mathbf{X})$ .

As shown in the Lemma 3.5, the nuclear norm can be reformulated in terms of factorized matrices [28]. Then we have

$$\begin{aligned} \min_{\mathbf{W}, \mathbf{H}} f(\mathbf{W}\mathbf{H}^\top) - \lambda \|\mathbf{W}\mathbf{H}^\top\|_F + \lambda/2(\|\mathbf{W}\|_F^2 + \|\mathbf{H}\|_F^2) \\ \geq \min_{\mathbf{X}} f(\mathbf{X}) - \lambda \|\mathbf{X}\|_F + \min_{\mathbf{W}, \mathbf{H}} \lambda/2(\|\mathbf{W}\|_F^2 + \|\mathbf{H}\|_F^2) \quad \text{s.t. } \mathbf{X} = \mathbf{W}\mathbf{H}^\top \\ \geq \min_{\mathbf{X}} f(\mathbf{X}) - \lambda \|\mathbf{X}\|_F + \lambda \|\mathbf{X}\|_*. \end{aligned}$$

Thus, if  $(\bar{\mathbf{W}}, \bar{\mathbf{H}})$  is a critical point of (7), then  $\bar{\mathbf{X}} = \bar{\mathbf{W}}(\bar{\mathbf{H}})^\top$  is also critical point of (1) with  $r(\mathbf{X}) = r_{\text{NNFN}}(\mathbf{X})$ .  $\square$

## B More on Experiments

Due to space limitation, we have to remove some details and results from the main text and present them here. In Section B.1, we introduce more details on setup of data and codes. Then in Section B.2, we present the full experimental results.

### B.1 Setup

#### B.1.1 Data

The statistics of the data sets used in the paper are listed in Table 5. All these data sets are public downloadable: *MovieLens*<sup>3</sup>; *Yahoo*<sup>4</sup>; *building* and *cabbage*<sup>5</sup>; *GAS*<sup>6</sup>; and *USHCN*<sup>7</sup>.

Table 5: Statistics on the real-world data sets. The first entry in brackets forms the row, and the second forms the column.

	<i>recommendation</i> (user, item)		<i>hyperspectral</i> (pixel, band)		<i>climate</i> (place, time-stamp)	
	<i>MovieLens</i>	<i>Yahoo</i>	<i>building</i>	<i>cabbage</i>	<i>GAS</i>	<i>USHCN</i>
number of rows	6,040	249,012	1,258,208	692,736	125	1,218
number of columns	3,449	296,111	49	49	156	1,211

**More Details on Hyperspectral Data** Hyperspectral images of *building* and *cabbage* from [33] are used. Each hyperspectral image originally has resolution  $I_1 \times I_2$  and  $I_3$  spectral bands, and is converted to a  $I_1 I_2 \times I_3$  matrix. The resultant *building* is of size  $1258208 \times 49$  and *cabbage* is of size  $692736 \times 49$ .

**More Details on Climate Data** The *GAS* and *USHCN* data sets from [1] are used. *GAS* contains monthly observations for the green gas components from January 1990 to December 2001. Here, we use the components  $CO_2$  and  $H_2$ . *USHCN* contains monthly temperature and precipitation readings from January 1919 to November 2019. For these two data sets, some rows (which correspond to locations) of the observed matrix are completely missing. To allow generalization to these completely unknown locations, we follow [1] and add a graph Laplacian regularizer to (1). Specifically, the  $m$  locations are represented as nodes on a graph. The affinity matrix  $\mathbf{A} = [A_{ij}] \in \mathbb{R}^{m \times m}$ , which contains pairwise node similarities, is computed as  $A_{ij} = \exp(-2b(i, j))$ , where  $b(i, j)$  is the Haversine distance between locations  $i$  and  $j$ . The graph Laplacian regularizer is then defined as  $a(\mathbf{X}) = \text{tr}(\mathbf{X}^\top (\mathbf{D} - \mathbf{A})\mathbf{X})$ , where  $D_{ii} = \sum_j A_{ij}$ . For the factorized models (LMaFit, BPFM and NNFN(factored)), we write  $a(\mathbf{X})$  as  $a(\mathbf{W}\mathbf{H}^\top)$ .

<sup>3</sup><http://grouplens.org/datasets/movielens/>

<sup>4</sup><http://webscope.sandbox.yahoo.com/catalog.php?datatype=c>

<sup>5</sup><https://sites.google.com/site/hyperspectralcolorimaging/dataset/>

<sup>6</sup><https://viterbi-web.usc.edu/~liu32/data/NA-1990-2002-Monthly.csv>

<sup>7</sup><http://www.ncdc.noaa.gov/oa/climate/research/ushcn>

### B.1.2 Compared Methods

For the methods that we compare in the experiments, we use their public available codes.

The low-rank regularizers compared include: (i) convex nuclear norm regularizer  $\|\mathbf{X}\|_*$  [6] optimized by the recent softImpute algorithm via alternating least squares<sup>8</sup> [15]; (ii) nonconvex low-rank regularizers of the form (3), including the capped- $\ell_1$  penalty [35], log-sum penalty (LSP) [8]; and minimax concave penalty (MCP) [34], is optimized by the recent low-rank matrix learning solver FaNCL<sup>9</sup> [33]; and (iii) truncated  $\ell_{1-2}$  regularizer in (4) [22] optimized with the difference of convex functions (DCA) algorithm with sub-problems solved by the alternating direction method of multipliers (ADMM)<sup>10</sup>.

The matrix factorization algorithms compared include: (i) low-rank matrix fitting algorithm (LMaFit)<sup>11</sup> [29], which directly solves  $\min_{\mathbf{W}, \mathbf{H}} f(\mathbf{W}\mathbf{H}^\top) + \frac{\lambda}{2}(\|\mathbf{W}\|_F^2 + \|\mathbf{H}\|_F^2)$ ; and (ii) Bayesian probabilistic matrix factorization (BPMF)<sup>12</sup> [23], which is a Bayesian model trained with Markov chain Monte Carlo [12].

All the algorithms are implemented in MATLAB, while sparse tensor and matrix operations are written in C as MEX functions.

For hyperparameter tuning,  $\lambda$  in (1) is chosen from  $[10^{-3}, 10^2]$ ,  $k$  is a integer chosen from  $[1, \min(m, n)]$ , and stepsize is chosen from  $[10^{-5}, 1]$ . For the other baselines, we use the hyperparameter ranges as mentioned in the corresponding papers. All hyperparameters are tuned by grid search using the validation set.

## B.2 Results

### B.2.1 Rank of the Recovered Matrix

In this section, we report the rank of the recovered matrix obtained by different methods on all the data sets used in Section 4.

Table 6 shows the rank obtained on synthetic data. As shown, all methods except the nuclear norm regularizer can recover the true rank value  $k^* = 5$ . Table 7 shows the rank obtained on real-world data. As can be seen, truncated  $\ell_{1-2}$ , NNFN(naive), NNFN(factored) LMaFit and BPMF obtain the same rank results. However, as shown in Table 9 and Table 10 below, the recovery performance of LMaFit and BPMF are worse. This may be explained by the adaptive penalization on singular values taken by nonconvex low-rank regularizers.

Table 6: Rank of the recovered matrix on the synthetic data.

	$m = 500$	$m = 1000$	$m = 2000$
LMaFit	5	5	5
BPMF	5	5	5
nuclear norm	108	61	77
capped- $\ell_1$	5	5	5
LSP	5	5	5
MCP	5	5	5
truncated $\ell_{1-2}$	5	5	5
NNFN(naive)	5	5	5
NNFN(factored)	5	5	5

Further, we examine the singular values obtained by LMaFit, BPMF and NNFN(factored), which optimize for factorized forms. The ground-truth singular values  $\sigma(\mathbf{G})$  are obtained by rank- $k^*$  truncated SVD on the clean data matrix  $\mathbf{G}$ , and the singular values of the recovered matrix are obtained by rank- $k^*$  truncated SVD on  $\tilde{\mathbf{X}} = \tilde{\mathbf{W}}\tilde{\mathbf{H}}^\top$  (where  $\tilde{\mathbf{W}}$  and  $\tilde{\mathbf{H}}$  are learned). The experiment is performed on the synthetic data set with  $m = 1000$ . Figure 4 plots the absolute value of the

<sup>8</sup>[https://cran.r-project.org/src/contrib/softImpute\\_1.4.tar.gz](https://cran.r-project.org/src/contrib/softImpute_1.4.tar.gz), we rewrite it in MATLAB

<sup>9</sup><https://github.com/quanmingyao/FaNCL>

<sup>10</sup><https://sites.google.com/site/louyifei/TL12-webcode.zip?attredirects=0&d=1>

<sup>11</sup><https://www.caam.rice.edu/~optimization/L1/LMaFit/download.html>

<sup>12</sup><https://www.cs.toronto.edu/~rsalakhu/BPMF.html>

difference between each  $\sigma_i(\mathbf{X})$  and  $\sigma_i(\mathbf{G})$ . As shown, LMaFit, BPMF and NNFN(factored) obtain different singular values. Among them, NNFN(factored) penalizes less on large singular values, and obtains singular values that are closer to the ground-truth singular values in  $\sigma(\mathbf{G})$ .

Table 7: Rank of the recovered matrix on the real-world data.

	<i>recommendation</i>		<i>hyperspectral</i>		<i>climate-GAS</i>		<i>climate-USHCN</i>	
	<i>MovieLens</i>	<i>Yahoo</i>	<i>building</i>	<i>cabbage</i>	<i>CO<sub>2</sub></i>	<i>H<sub>2</sub></i>	<i>temper.</i>	<i>precip.</i>
LMaFit	9	6	1	3	10	10	3	5
BPMF	9	6	1	3	10	9	3	5
nuclear norm	27	-	49	49	8	7	35	121
capped- $\ell_1$	8	8	1	3	5	10	6	10
LSP	9	9	1	3	4	8	5	5
MCP	7	7	1	3	9	3	3	5
truncated $\ell_{1-2}$	5	-	1	3	9	10	3	5
NNFN(naive)	5	-	1	3	9	10	3	5
NNFN(factored)	5	6	1	3	9	10	3	5

Figure 4: Absolute difference in singular values  $|\sigma_i(\tilde{\mathbf{X}}) - \sigma_i(\mathbf{G})|$  for each  $i$  on the synthetic data set ( $m = 1000$ ). Here,  $\tilde{\mathbf{X}}$  is the recovered matrix, and  $\mathbf{G}$  is the ground-truth matrix (Section 4.2).

### B.2.2 Effects of Noise, Rank and Sparsity Ratio on Synthetic Data

Corresponding to the examination on how noise, rank and sparsity ratio affect learning performance in Section 4.2, the timing results are shown in Figure 5. Although the exact timing results vary across different settings, the trend remains the same as observed in the main text. NNFN(factored) is consistently the fastest, and truncated  $\ell_{1-2}$  is the slowest.

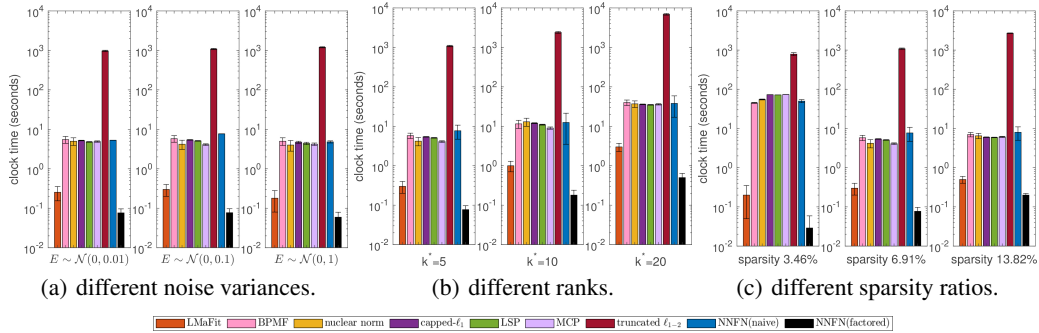


Figure 5: Clock time (seconds) obtained with different settings on the synthetic data set ( $m = 1000$ ).

### B.2.3 Full Performance Table

As mentioned in Section 4, all experimental results are averaged over five runs. In the main text, we only report the average performance due to space limitation. Here we provide results recorded as "mean  $\pm$  standard deviation" for both recovery error in terms of RMSE or NMSE and the training clock time.

Tables 8 and 10 below correspond to Tables 2 and 3 in the main text, while Table 9 shows the results on recommendation data and hyperspectral images. As can be seen, NNFN(factored) always obtains the best performance, and nonconvex regularizers are better than LMaFit, BPMF and nuclear norm regularizer in general.

Table 8: Performance on the synthetic data with different dimensionalities ( $m$ 's). For each data set, its sparsity ratio is shown in brackets. Error is the testing NMSE scaled by  $10^{-2}$ . The best and comparable results (according to the pairwise t-test with 95% confidence) are highlighted in bold.

	$m = 500$ (12.43%)		$m = 1000$ (6.91%)		$m = 2000$ (3.80%)	
	error	time (s)	error	time (s)	error	time (s)
LMaFit	$2.46 \pm 0.03$	$0.08 \pm 0.02$	$2.18 \pm 0.04$	$0.3 \pm 0.1$	$1.98 \pm 0.01$	$1.5 \pm 0.2$
BPMF	$2.34 \pm 0.05$	$3.2 \pm 0.4$	$2.03 \pm 0.05$	$5.8 \pm 0.9$	$1.88 \pm 0.01$	$48.3 \pm 5.9$
nuclear norm	$4.36 \pm 0.03$	$2.1 \pm 0.2$	$3.75 \pm 0.03$	$4.2 \pm 1.0$	$3.33 \pm 0.01$	$40.9 \pm 7.2$
capped- $\ell_1$	<b><math>1.97 \pm 0.03</math></b>	$0.8 \pm 0.1$	<b><math>1.83 \pm 0.03</math></b>	$5.4 \pm 0.1$	<b><math>1.78 \pm 0.01</math></b>	$36.0 \pm 3.4$
LSP	<b><math>1.97 \pm 0.03</math></b>	$0.8 \pm 0.1$	<b><math>1.83 \pm 0.04</math></b>	$5.1 \pm 0.1$	<b><math>1.77 \pm 0.01</math></b>	$35.1 \pm 2.1$
MCP	<b><math>1.96 \pm 0.03</math></b>	$0.7 \pm 0.1$	<b><math>1.82 \pm 0.03</math></b>	$4.1 \pm 0.2$	<b><math>1.78 \pm 0.01</math></b>	$40.6 \pm 3.6$
truncated $\ell_{1-2}$	<b><math>1.96 \pm 0.03</math></b>	$695.8 \pm 19.2$	<b><math>1.82 \pm 0.04</math></b>	$1083.2 \pm 40.78$	<b><math>1.77 \pm 0.01</math></b>	$3954.1 \pm 98.7$
NNFN(naive)	<b><math>1.96 \pm 0.03</math></b>	$2.1 \pm 0.2$	<b><math>1.82 \pm 0.03</math></b>	$7.7 \pm 0.6$	<b><math>1.77 \pm 0.01</math></b>	$43.1 \pm 2.3$
NNFN(factored)	<b><math>1.96 \pm 0.03</math></b>	<b><math>0.04 \pm 0.01</math></b>	<b><math>1.82 \pm 0.03</math></b>	<b><math>0.08 \pm 0.02</math></b>	<b><math>1.77 \pm 0.01</math></b>	<b><math>0.3 \pm 0.1</math></b>

Table 9: Performance on the recommendation and hyperspectral data. Error is RMSE scaled by  $10^{-1}$ . Entries marked as “-” mean that the corresponding methods cannot complete in three hours. The best and comparable results (according to the pairwise t-test with 95% confidence) are highlighted in bold.

	recommendation				hyperspectral			
	<i>MovieLens</i>		<i>Yahoo</i>		<i>building</i>		<i>cabbage</i>	
	error	time (s)	error	time (s)	error	time (s)	error	time (s)
LMaFit	8.10 $\pm 0.01$	25.3 $\pm 3.7$	7.10 $\pm 0.08$	860.3 $\pm 33.1$	0.54 $\pm 0.01$	12.6 $\pm 0.6$	0.49 $\pm 0.01$	11.5 $\pm 1.7$
BPMF	8.07 $\pm 0.01$	215.3 $\pm 29.4$	7.07 $\pm 0.03$	1433.5 $\pm 89.2$	0.53 $\pm 0.01$	370.5 $\pm 7.3$	0.49 $\pm 0.01$	183.6 $\pm 6.2$
nuclear norm	8.20 $\pm 0.02$	118.7 $\pm 19.2$	-	-	0.56 $\pm 0.01$	277.1 $\pm 12.1$	0.53 $\pm 0.01$	133.7 $\pm 2.1$
capped- $\ell_1$	8.00 $\pm 0.01$	147.9 $\pm 23.3$	6.58 $\pm 0.01$	1296.8 $\pm 67.3$	<b>0.50</b> $\pm 0.01$	264.8 $\pm 4.6$	<b>0.46</b> $\pm 0.01$	79.2 $\pm 3.2$
LSP	7.99 $\pm 0.01$	149.2 $\pm 23.5$	6.56 $\pm 0.01$	1078.0 $\pm 69.0$	<b>0.50</b> $\pm 0.01$	274.4 $\pm 25.4$	<b>0.46</b> $\pm 0.01$	150.5 $\pm 3.1$
MCP	8.01 $\pm 0.01$	151.4 $\pm 23.9$	6.78 $\pm 0.01$	1108.3 $\pm 41.4$	<b>0.50</b> $\pm 0.01$	266.7 $\pm 9.8$	<b>0.46</b> $\pm 0.01$	144.2 $\pm 2.9$
truncated $\ell_{1-2}$	<b>7.97</b> $\pm 0.01$	6068.4 $\pm 172.0$	-	-	<b>0.50</b> $\pm 0.01$	9836.1 $\pm 470.4$	<b>0.46</b> $\pm 0.01$	6934.2 $\pm 190.1$
NNFN(naive)	<b>7.97</b> $\pm 0.01$	134.2 $\pm 19.6$	-	-	<b>0.50</b> $\pm 0.01$	295.5 $\pm 11.3$	<b>0.46</b> $\pm 0.01$	82.9 $\pm 2.0$
NNFN(factored)	<b>7.97</b> $\pm 0.01$	<b>0.5</b> $\pm 0.1$	<b>6.52</b> $\pm 0.01$	<b>522.5</b> $\pm 21.9$	<b>0.50</b> $\pm 0.01$	<b>6.2</b> $\pm 0.5$	<b>0.46</b> $\pm 0.01$	<b>3.6</b> $\pm 0.4$

Table 10: Performance on the climate data sets. Error is RMSE scaled by  $10^{-1}$ . The best and comparable results (according to the pairwise t-test with 95% confidence) are highlighted in bold.

	GAS				USHCN			
	$CO_2$		$H_2$		temperature		precipitation	
	error	time(s)	error	time(s)	error	time(s)	error	time(s)
LMaFit	5.65 $\pm 0.06$	0.17 $\pm 0.02$	5.74 $\pm 0.05$	0.19 $\pm 0.03$	4.83 $\pm 0.16$	15.7 $\pm 2.4$	8.23 $\pm 0.18$	33.3 $\pm 1.7$
BPMF	5.52 $\pm 0.05$	3.2 $\pm 0.3$	5.54 $\pm 0.05$	3.4 $\pm 0.4$	4.64 $\pm 0.12$	148.1 $\pm 7.7$	8.19 $\pm 0.15$	125.1 $\pm 8.1$
nuclear norm	5.84 $\pm 0.05$	1.0 $\pm 0.1$	5.93 $\pm 0.06$	0.8 $\pm 0.1$	4.80 $\pm 0.14$	108.5 $\pm 4.1$	8.28 $\pm 0.20$	84.9 $\pm 11.2$
capped- $\ell_1$	5.33 $\pm 0.03$	0.6 $\pm 0.1$	<b>5.31</b> <b><math>\pm 0.05</math></b>	0.7 $\pm 0.2$	4.50 $\pm 0.14$	108.5 $\pm 10.5$	<b>8.06</b> <b><math>\pm 0.14</math></b>	87.2 $\pm 6.2$
LSP	5.37 $\pm 0.08$	1.2 $\pm 0.1$	5.40 $\pm 0.07$	1.3 $\pm 0.2$	4.48 $\pm 0.10$	133.3 $\pm 7.7$	<b>8.06</b> <b><math>\pm 0.14</math></b>	105.8 $\pm 7.4$
MCP	<b>5.30</b> <b><math>\pm 0.08</math></b>	1.0 $\pm 0.1$	5.34 $\pm 0.06$	0.5 $\pm 0.1$	<b>4.44</b> <b><math>\pm 0.13</math></b>	92.5 $\pm 6.1$	<b>8.06</b> <b><math>\pm 0.14</math></b>	85.2 $\pm 7.3$
truncated $\ell_{1-2}$	<b>5.30</b> <b><math>\pm 0.07</math></b>	11.0 $\pm 1.2$	<b>5.31</b> <b><math>\pm 0.05</math></b>	7.3 $\pm 1.8$	<b>4.44</b> <b><math>\pm 0.13</math></b>	573.9 $\pm 18.1$	<b>8.06</b> <b><math>\pm 0.14</math></b>	318.5 $\pm 9.7$
NNFN(naive)	<b>5.30</b> <b><math>\pm 0.08</math></b>	0.4 $\pm 0.1$	<b>5.31</b> <b><math>\pm 0.05</math></b>	0.5 $\pm 0.1$	<b>4.44</b> <b><math>\pm 0.12</math></b>	57.1 $\pm 3.3$	<b>8.06</b> <b><math>\pm 0.14</math></b>	66.4 $\pm 5.1$
NNFN(factored)	<b>5.30</b> <b><math>\pm 0.06</math></b>	<b>0.05</b> <b><math>\pm 0.01</math></b>	<b>5.31</b> <b><math>\pm 0.05</math></b>	<b>0.05</b> <b><math>\pm 0.02</math></b>	<b>4.44</b> <b><math>\pm 0.12</math></b>	<b>5.9</b> <b><math>\pm 1.4</math></b>	<b>8.06</b> <b><math>\pm 0.15</math></b>	<b>13.5</b> <b><math>\pm 1.9</math></b>

## B.2.4 Convergence Plot

Figure 6 shows the convergence of RMSE on data sets that are removed from the main text due to space limitation. As shown, nonconvex regularizers generally obtain better testing RMSEs. Among them, NNFN(factored) is the fastest in convergence. This validates the efficiency and effectiveness of NNFN(factored).

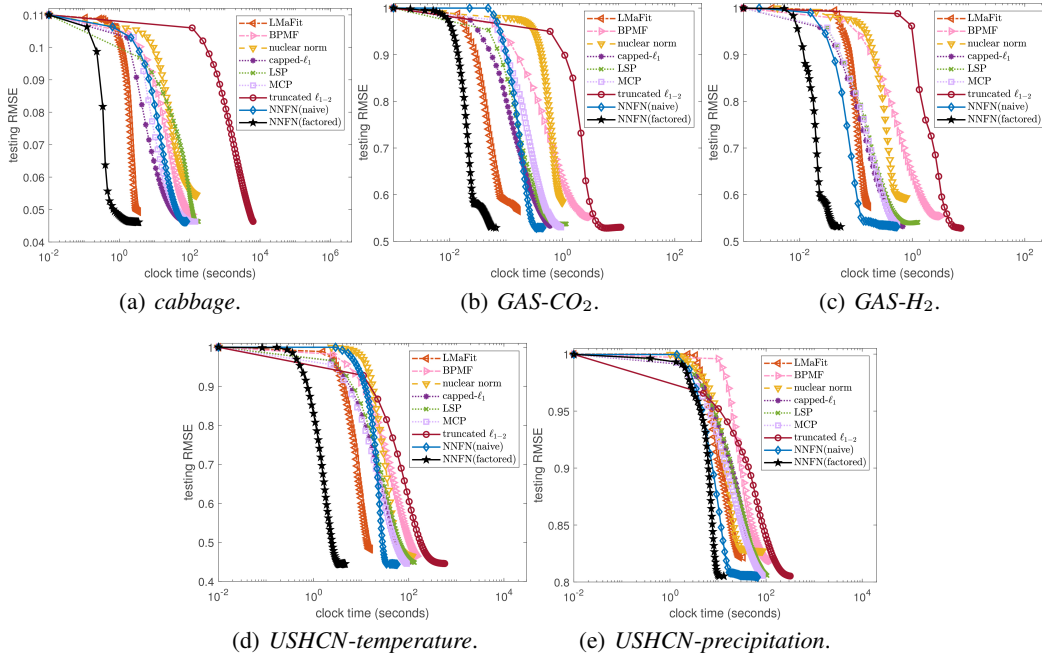


Figure 6: Testing RMSE versus clock time on the data sets not reported in the main text.